Experimental Results Using a Sliding Mode Brake Controller with Non-smooth Adaptation

Michael Uchanski† , Massimiliamo Gobbi‡ , Rick Hill , JK Hedrick
Department of Mechanical Engineering
University of California, Berkeley
Berkeley, California, USA

Abstract— **We design and experimentally demonstrate a sliding mode brake controller which allows an automated vehicle to precisely follow speed profiles. The gain between the brake pressure and brake torque can change significantly due to temperature and other factors, so two different Lyapunov-based adaptation laws—one "smooth" and the other "nonsmooth"—are designed to compensate. The smooth adaptation law derives from a standard quadratic Lyapunov function, and the nonsmooth one comes from a Lyapunov function which is not smooth at the origin. Experiments using a strain-based brake torque sensor show that both adaptation algorithms reduce tracking error and converge to the correct parameter values.**

I. Introduction

"Brake fade"—the situation where elevated temperatures at the brake rotor decrease braking gain—is a phenomenon which most drivers have experienced. In an automated highway, or short-headway automated cruise control, even a moderate change in the brake system gain could lead to unacceptable tracking errors. Even if tracking errors are acceptable, it is often desirable to know the brake system gain in order to estimate other parameters. For example, [2] introduces a novel road friction force observer which requires an estimate of the brake gain to give quantitatively accurate results.

Here, we develop and experimentally demonstrate two versions of an adaptive sliding mode brake controller which compensates for an unknown brake gain. One of the algorithms, originally presented by Maciuca [3] uses the concept of nonsmooth Lyapunov functions [5] to derive an adaptation law which may have more desirable convergence properties than standard adaptation laws.

The remainder of this paper is organized as follows: Section II introduces the vehicle model and derives a sliding mode controller. Section III then introduces two adaptive algorithms—one "smooth," and one "non-smooth"—to compensate for the unknown brake pressure to brake torque gain. The smooth algorithm arises out of a standard quadratic Lyapunov function, and the nonsmooth algorithm is derived from a Lyapunov function with a discontinuous derivative at the origin. In Section IV a test vehicle with a strain based brake torque sensor is used to experimentally verify the stability and parameter convergence of the adaptive controller. Finally, Section V offers conclusions and directions for future work.

†email: mikeu@vehicle.me.berkeley.edu
‡Massimiliamo Gobbi was a visiting researcher at UC Berkeley and is currently with the Dip. di Meccanica, Politecnico di Milano, Italy.

II. Vehicle Model and Control Algorithm

In this section, we present a simplified longitudinal vehicle model and derive a brake controller for velocity profile tracking.

A. Vehicle Model

An $F = ma$ force balance for the vehicle results in the equation

$$F_{x_f} + F_{x_r} - F_d = ma_x \tag{1}$$

with

F_{x_f}	road force on the front wheels
F_{x_r}	road force on the rear wheels
F_d	drag forces due to wind and grade
m	vehicle mass including wheels

Moment balances for the front (not connected to engine) and rear (connected to engine) wheels give

$$J_{w_f}\dot{\omega}_{w_f} = -rF_{x_f} - M_f - T_{b_f} \tag{2}$$

and

$$J_r\dot{\omega}_r = T_e - rF_{x_r} - M_r - T_{b_r} \tag{3}$$

with

J_{w_f}	moment of inertia of front wheels
J_r	J of rear wheels, differential, engine, gears
M_f	front wheel rolling resistance moment
M_r	rear wheel rolling resistance moment
T_{b_f}	front brake rotor torque
T_{b_r}	rear brake rotor torque
T_e	torque converter output torque as seen at wheel
F_{x_f}	road force on the front wheels, as above
F_{x_r}	road force on the rear wheels, as above
r	wheel radius

The moment balance for the rear wheel assumes that the entire drive train can be treated as one lumped inertia. Although this is not true in general, especially under high torque conditions, it is a reasonable approximation for generating a relatively simple control-oriented model.

If we assume wheel slip to be negligible, then the kinematic rolling condition gives that $\dot{\omega}_{w_f} = \dot{\omega}_{w_r} = a/r$, and we can solve equations 2 and 3—the torque balances at the wheel—for F_{x_f} and F_{x_f}, substitute into the $F = ma$ equation for the vehicle (equation 1), and group terms multiplying a to yield

$$[T_e - T_{b_f} - T_{b_r} - M_f - M_r]/r - F_d = \left(m + \frac{J_{w_f} + J_r}{r^2}\right) a \tag{4}$$

If we group the brake torques T_{b_f} and T_{b_r} together into one effective brake torque T_b, lump the rolling resistance moments into an effective rolling resistance moment M, and substitute $J_{w_r} + \frac{J_e}{R_g^2}$ (R_g is the ratio of the wheel rotational speed to the engine rotational speed, J_e is the moment of inertia of the engine, and J_{w_r} is the moment of inertia of the rear wheels) for the lumped wheel/drivetrain/engine inertia J_r, we get

$$\frac{T_e - T_b - M}{r} - F_d = \left(m + \frac{J_{w_r} + \frac{J_e}{R_g^2} + J_{w_f}}{r^2} \right) a \quad (5)$$

which simplifies to

$$T_e - T_b - M - rF_d = \frac{1}{R_g^2} \left(J_e + R_g^2 (mr^2 + J_{w_r} + J_{w_f}) \right) a \quad (6)$$

Defining $\beta = \frac{1}{R_g^2} \left(J_e + R_g^2 (mr^2 + J_{w_r} + J_{w_f}) \right)$ gives

$$T_e - T_b - M - rF_d = \beta a \quad (7)$$

Finally, if we model the drag force as a "velocity-squared" phenomenon with coefficient of drag C, so that $F_d = Cv^2$, we get

$$T_e - T_b - M - rCv^2 = \beta a \quad (8)$$

as our final equation of motion for the vehicle. To simplify notation in the following sections, we define $T_{ext} = T_e - M - rCV^2$ to be the sum of the engine, rolling resistance, and wind drag terms to get

$$T_{ext} - T_b = \beta a \quad (9)$$

Equation 9 serves as the basis of our longitudinal control and parameter adaptation algorithms in the following sections.

B. Brake Controller

Using the vehicle model developed above, we now design a velocity tracking brake controller which we will augment in the next section with adaptation. An engine controller and switching logic between throttle and brakes have been previously designed, but are omitted here for brevity.

Unfortunately, the control input for the brakes is not the T_b appearing in the vehicle's equation of motion, $T_{ext} - T_b = \beta a$. Instead, the input is the brake pressure at the master cylinder which, neglecting brake cylinder "pushout pressure" and hydraulic dynamics and assuming low slip, is linearly related to the brake torque:

$$T_b = K_b u \quad (10)$$

Until brake pressures are large enough to cause wheel lockup, the linearity assumption is quite good. However, the gain, K_b, can change by more than 50% under normal driving conditions. A change in the gain due to heat is commonly called "brake fade" and is a noticeable, even dangerous, problem on long downhill sections of road. Water and brake pad wear can also significantly affect the brake gain. For now, we proceed to design the control law assuming that the gain, K_b, is known and then introduce adaptation in the next section to compensate for its excursions from the nominal value.

The surface is defined to be the velocity error, so that when the controller reaches $S = 0$ we have that $v = v_{des}$:

$$S := v - v_{des} \quad (11)$$

To assure that the surface will reach zero, the control, u, is chosen so that the time derivative of a Lyapunov function $V := \frac{1}{2}S^2$ along the closed-loop state trajectories is negative, ie

$$S\dot{S} \leq 0 \quad (12)$$

Often, u is chosen with a switching term to assure that $S = 0$ is reached, but to avoid the chattering problems often associated with the switching term, we use an asymptotic approximation to sliding mode and choose u so that for $\lambda > 0$, $\dot{S} = -\lambda S$, giving $\dot{V} = -\lambda S^2$. To find the control, we substitute the vehicle dynamics of equation 9 into the desired surface dynamics $\dot{S} = -\lambda S$:

$$\dot{S} = \dot{v} - \dot{v}_{des} = \frac{T_{ext} - K_b u}{\beta} - \dot{v}_{des} = -\lambda S \quad (13)$$

Solving for u gives the rule for choosing brake pressure:

$$u = \frac{1}{K_b} (T_{ext} + \beta(\lambda S - \dot{v}_{des})) \quad (14)$$

III. Adaptation Algorithms

A myriad of factors—among them temperature, pad material, wear, and moisture—can profoundly affect the gain K_b used in the control law of equation 14, leading to unacceptable tracking errors. Thus, two schemes to adapt on the value of K_b were designed. The "smooth" formulation follows a standard design process, and is used as a benchmark. The "nonsmooth" formulation uses the theory of nonsmooth Lyapunov functions and is of interest because it may offer better parameter convergence.

A. Smooth K_b Adaptation

Adding dynamics to the estimated brake torque gain, $\hat{K}_b$, makes the system two states instead of one, so we construct a Lyapunov function, V_1, out of the velocity error, S, and the parameter error, $\tilde{K}_b := K_b - \hat{K}_b$, both of which we would like to make stable :

$$V_1 = \frac{1}{2}S^2 + \frac{\gamma}{2}\tilde{K}_b^2 \quad (15)$$

Taking the time derivative and substituting the definition of S gives

$$\dot{V}_1 = S(\dot{v} - \dot{v}_{des}) - \gamma \tilde{K}_b \dot{\hat{K}}_b \quad (16)$$

Employing equation 9—the vehicle equation of motion—and using the control law of equation 14 with our current estimate of the torque gain, $\hat{K}_b$, replacing K_b yields

$$\dot{V}_1 = S \left(\frac{1}{\beta}(T_{ext} - \frac{K_b}{\hat{K}_b} T_{ext} - \frac{K_b}{\hat{K}_b}\beta(\lambda S - \dot{v}_{des})) - \dot{v}_d es \right) - \gamma \tilde{K}_b \dot{\hat{K}}_b \quad (17)$$

Using the identity $\frac{K_b}{\hat{K}_b} = \frac{\tilde{K}_b}{\hat{K}_b} + 1$ and assuming that K_b varies slowly so that $\dot{\tilde{K}}_b = -\dot{\hat{K}}_b$ gives

$$\dot{V}_1 = -\lambda S^2 - \frac{S\tilde{K}_b}{\hat{K}_b} \left(\frac{1}{\beta} T_{ext} + \lambda S - \dot{v}_{des} \right) - \gamma \tilde{K}_b \dot{\hat{K}}_b \quad (18)$$

so that choosing

$$\dot{\hat{K}}_b = -\frac{S}{\gamma \hat{K}_b} \left(\frac{1}{\beta} T_{ext} + \lambda S - \dot{v}_{des} \right) \quad (19)$$

gives $\dot{V}_1 = -\lambda S^2$, implying that V_1 does not grow. This, combined with the fact that V_1 is radially unbounded, allows us to conclude that S and $\tilde{K}_b$ are bounded. To show that S goes to zero, we first calculate $\ddot{V}_1 = 2\lambda^2 S^2$. Since S is bounded $\ddot{V}_1$ also is, implying that $\dot{V}$ is uniformly

continuous. Since V is lower bounded by zero and negative semidefinite and $\dot{V}$ is uniformly continuous, Barbalat's lemma can be used to conclude that $\dot{V} \to 0$ so $S \to 0$. Convergence of $\tilde{K}_b$ is achieved if the system is persistently excited.

B. Non-Smooth K_b Adaptation

A nonsmooth adaptation algorithm for $\hat{K}_b$ was also derived using a similar procedure, but starting with a nonsmooth Lyapunov function:

$$V_2 := Ssgn(S) + \frac{\gamma}{2}\tilde{K}_b^2 \tag{20}$$

The same procedure as above holds everywhere except at $S = 0$ where the $sgn(\cdot)$ function is not defined, giving the adaptation law

$$\dot{\hat{K}}_b = -\frac{sgn(S)}{\hat{K}_b}\left(\frac{1}{\beta}T_{ext} + \lambda S - \dot{v}_d\right) \tag{21}$$

Stability analysis is complicated by the slope discontinuity in the Lyapunov function at zero and proceeds according to an extension to Lyapunov theory which the treats derivative of the Lyapunov function at this point as the convex closure of the derivatives on either side. More detailed treatment of these concepts can be found in Maciuca [3] and in Shevitz and Paden [5].

IV. Experiments on Vehicle

The controller and adaptive algorithms developed in the previous section were tested on a 1990 Lincoln Towncar belonging to the California PATH program automated highway program. The test vehicle is equipped with a data acquisition and control computer, strain-based brake torque sensor, throttle actuator, brake pressure actuator, wheel speed sensors, manifold pressure sensors, and differential braking capabilities.

In addition to monitoring velocity tracking error, we used the torque sensor to check that the adaptive controller's estimate of the brake torque given by $\hat{K}_b u$ corresponded to the actual torque, indicating that the parameter $\hat{K}_b$ had converged to the correct value.

Unfortunately, the strain-based torque sensor was only installed on the vehicle's *left front wheel*, while the adaptive algorithms developed in the previous section estimate the gain between the brake system pressure and the *total* brake torque on the vehicle—from all four brakes. To assure that the total brake torque on the vehicle equaled the left front wheel torque, braking to the other three wheels was disabled by over-riding the vehicle's ABS controller. The non-symmetrical braking caused a small yaw moment on the vehicle, but decelerations were kept low enough for it to have no noticeable effect.

The same trapezoidal profile for the desired velocity, v_{des}, was used in each test: The vehicle started at 6 m/s and maintained this speed until $t = 5s$, at which point it accelerated for $7.5s$ at $0.8m/s^2$ to reach $12m/s$. It then maintained this speed for $5s$ before decelerating at $0.8m/s^2$ for $7.5s$ to return to $6m/s$. Braking occurs only between $t = 17.5$ and $t = 25$.

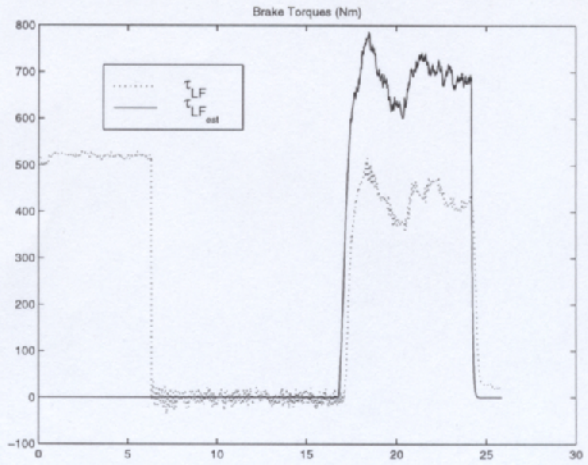

Fig. 1. Measured and estimated brake torque for baseline test with no adaptation. The initial high value of the measured brake torque is an artifact of the offset removal scheme used for the sensor.

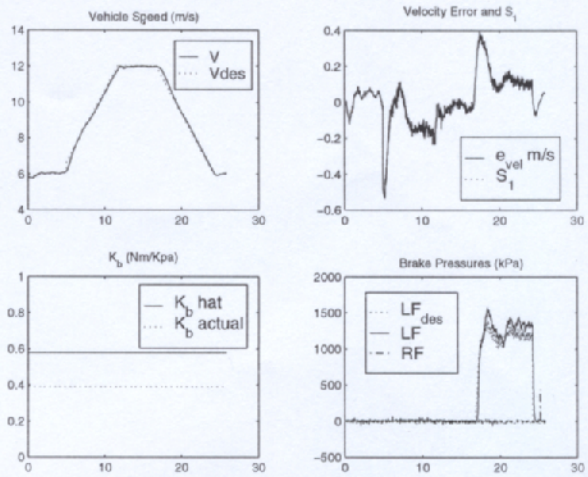

Fig. 2. Results of baseline test with no adaptation.

A. Nonadaptive Controller

The first test demonstrates tracking performance of the controller developed in Section II without parameter adaptation. The actual value of K_b is $0.39\frac{Nm}{kPa}$, but the value which the controller uses is 50% too high at $0.58\frac{Nm}{kPa}$. The surface is the velocity error: $S := v - v_{des}$.

The upper left plot of Figure 2 shows the velocity tracking maneuver. Figure 1 shows that, due to the erroneous brake torque gain, the brake torque value which the controller uses is significantly higher than the actual torque. This results in a velocity tracking error of approximately $0.2\frac{m}{s}$, as shown in the upper right of Figure 2.

B. Smooth Adaptation

The second test demonstrates tracking performance with smooth parameter adaptation. Like before, the actual value of K_b is $0.39\frac{Nm}{kPa}$, but the value which the controller uses is 50% too high at $0.58\frac{Nm}{kPa}$. The surface in the sliding controller is just the velocity error: $S_1 := v - v_{des}$.

Figure 3 shows that the estimated torque converges to-

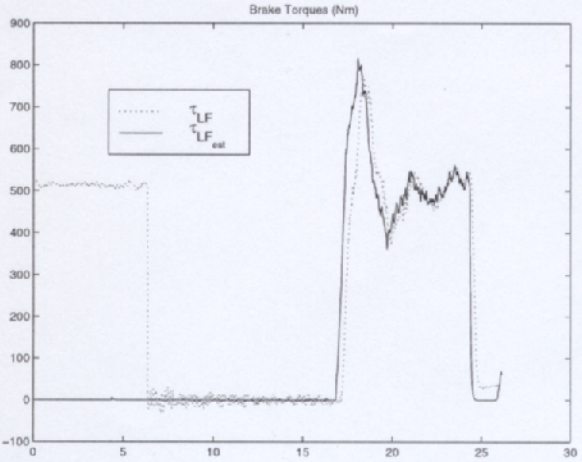

Fig. 3. Measured and estimated torques using smooth adaptive control law to adjust value of $\hat{K}_b$ and surface definition $S_1 := v - v_{des}$.

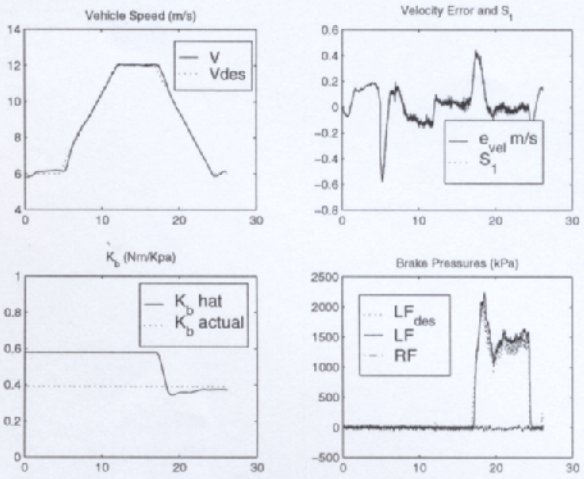

Fig. 4. Results of smooth $\hat{K}_b$ adaptation with $S_1 := v - v_{des}$.

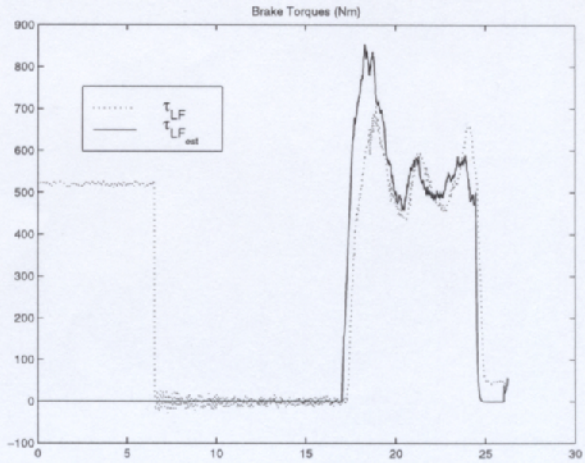

Fig. 5. Measured and estimated torques using switching adaptive control law to adjust value of $\hat{K}_b$ and surface definition $S_1 := v - v_{des}$.

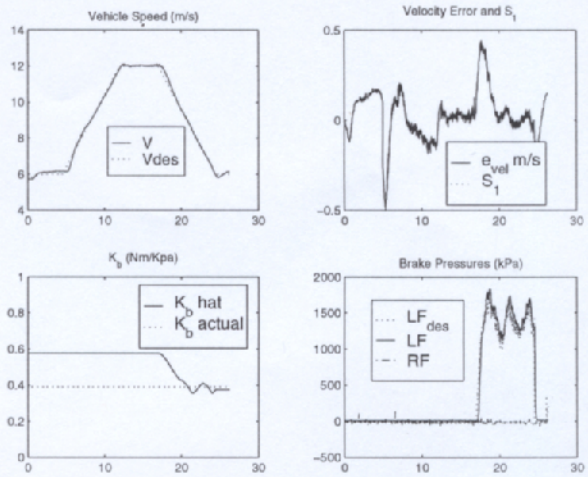

Fig. 6. Results of switching $\hat{K}_b$ adaptation with $S_1 := v - v_{des}$.

wards the measured value, and the upper right plot Figure 4 shows that the velocity error converges to zero and the parameter $\hat{K}_b$ converges. When the initial estimate of the brake torque gain differed by a large amount (a factor of three or four) from the actual brake torque gain, the parameter estimate, $\hat{K}_b$, sometimes would overshoot before converging to the correct value, causing uncomfortable oscillations in the brake pressure.

C. Non-Smooth Adaptation

The final test demonstrates tracking performance with nonsmooth parameter adaptation. As above, the actual value of K_b is $0.39\frac{Nm}{kPa}$, but the value which the controller uses is 50% too high at $0.58\frac{Nm}{kPa}$.

Figure 5 shows that the estimated torque converges towards the measured value, and Figure 6 shows that the velocity error converges to zero and the parameter $\hat{K}_b$ converges. When the initial parameter error was large, the uncomfortable oscillations which were present for the smooth parameter adaptation law did not occur.

Interesting behavior occurs once the parameter converges to the correct value. Due to modeling uncertainties, the parameter "chatters" around the correct value at a very low frequency. As a result, the surface also shows very low frequency chattering. The chattering was invisible to passengers and, in cases with many parameters, could prove to be beneficial by providing excitation to force convergence.

V. Conclusions

The non-adaptive sliding mode brake controller performed well but showed a tracking error when there were parameter mismatches. Although this could be remedied with a higher surface gain, an integral term in the surface, or a switching term, it would likely be at the expense of increased control effort.

Both adaptive algorithms reduced velocity tracking error and had their parameters converge to the correct value. The smooth adaptation scheme converged as expected, and the nonsmooth adaptation algorithm converged in a linear matter, chattering at a low frequency once it reached correct parameter value. For this application, the nonsmooth parameter adaptation law gave better results because it

had less of a tendency to over/undershoot the correct parameter value when the initial parameter error was large.

An interesting future direction for work would be to compare the convergence properties of the nonsmooth adaptation algorithm with those of the smooth adaptation algorithm in cases where persistence of excitation is difficult to achieve.

References

[1] J.P. Aubin and A. Cellina. *Differential Inclusions.* Springer-Verlag, 1984.

[2] Sergey Drakunov, Ümit Özgüner, Peter Dix, and Behrouz Ashrafi. Abs control using optimum search via sliding modes. *IEEE Transactions on Control Systems Technology*, 1995.

[3] Dragos Bogdan Maciuca. *Nonlinear Robust Control with Applications to Brake Control for Automated Highways.* PhD thesis, University of California Berkeley, 1997.

[4] Marques Monteiro and D.P. Manuel. *Differential Inclusions in Nonsmooth Mechanical Problems.* Birkhäuser, 1993.

[5] Daniel Shevitz and Brad Paden. Lyapunov stability theory of nonsmooth systems. In *Advances in Robust and Nonlinear Control Systems.*

[6] Jean-Jacques E. Slotine and Weiping Li. *Applied Nonlinear Control.* Prentice Hall, 1991.